GOSPODARKA SUROWCAMI MINERALNYMI – MINERAL RESOURCES MANAGEMENT

2024 Volume 40 Issue 3 Pages 69–86

DOI: 10.24425/gsm.2024.151525

SHUHAO HAO[1], GAIPIN CAI[2], WEIFENG WANG[3], LONGHUI FAN[3], XIN CAO[3]

Fractal characteristics analysis of ore-particle clusters under quasi-static loading

Introduction

With the proposal of carbon peak and carbon neutrality goals, scholars are increasingly focusing on how to achieve better energy conservation, emission reduction and enhanced resource utilization. The processing of ores involves multiple stages of crushing and grinding to meet subsequent processing requirements. The processes of crushing and grinding aim to reduce the particle size of raw ore materials to the desired specifications. However, a significant amount of energy is often wasted in this process. Therefore, investigating more efficient methods for ore crushing is of paramount importance for improving ore-fragmentation efficiency and achieving energy conservation and emission reduction.

✉ Corresponding Author: Shuhao Hao; e-mail: haoshuhao369@163.com

[1] School of Mechanical and Electrical Engineering, Jiangxi University of Science and Technology, China; ORCID iD: 0009-0007-7814-4302; e-mail: haoshuhao369@163.com

[2] School of Mechanical and Electrical Engineering, Jiangxi University of Science and Technology, China; Jiangxi Province Engineering Research Center for Mechanical and Electrical of Mining and Metallurgy, China; e-mail: 1123615286@qq.com

[3] School of Mechanical and Electrical Engineering, Jiangxi University of Science and Technology, China

Scholars have conducted extensive research on various factors, including experiments and simulations, related to the fragmentation of ore-particle clusters. Zhang et al. established a model for the cyclic compression crushing operation of granular materials, incorporating selection functions, crushing functions and particle-shape transformation functions, and subsequently solved the model (Zhang et al. 2017). Liu et al. employed numerical simulation using uniaxial compression to investigate the fragmentation process of particle clusters, obtaining simulated post-crushing particle distribution curves (Liu et al. 2005). Evertsson et al. through ore granular material crushing experiments, identified the correlation between crushing functions, selection functions, and the compression state of ore granular materials, leading to the development of an ore granular material cyclic compression crushing model (Evertsson and Bearman 1997). Nguyen et al. explored the impact of crushing energy on the effectiveness of fragmentation through unconfined quasi-static particle bed compression experiments (Nguyen et al. 2002). Liu et al. established a interparticle breakage model by analyzing particle bed crushing experiments with a narrow size distribution and developed a predictive method for inter-particle breakage results under different feed sizes (Liu and Schönert 1996). Liu considering the characteristics of the granular material size distribution, established a particle size model for cyclic compression based on the overall balance model (Liu 2020). Jiménez-Herrera et al. compared three particle fragmentation simulation models–FBM, BPM and PRM–and found that the PRM fragmentation simulation model demonstrated higher accuracy in post-crushing particle size distribution (Jiménez-Herrera et al. 2017). In the realm of mineral fractal characteristics, scholars have also conducted relevant research. Ning et al. studied the fractal characteristics of coal fatigue failure under low-frequency cyclic loading through a series of experiments and established the relationship between fractal dimension and fragment size, mass and quantity (Ning et al. 2018). Wang et al. utilizing a split Hopkinson pressure bar (SHPB) impact experiment system and applying fractal theory, investigated the fractal characteristics of the pore structure of coal before and after impact, revealing the influence of the impact load on the microscopic pore structure of anthracite coal (Wang and Liang 2020). Cai et al. employed fractal theory to establish a predictive model for energy consumption in low-frequency vibration and compression crushing of ores (Cai et al. 2016). Liu et al. researched the impact of loading rates on the fractal characteristics of rock fragmentation under impact loading (Liu et al. 2013). Wu et al. employed a split Hopkinson pressure bar to apply dynamic loads to laminated shale, obtaining the dynamic compressive strength and macroscopic failure modes of laminated shale under different bedding angles (Wu and Li 2019). In summary, scholars have conducted extensive research on the fragmentation of ore-particle clusters and mineral fractal dimension. However, there is a scarcity of reported studies on the analysis characteristics of simulation and the simulation of ore-particle cluster fragmentation.

In conventional comminution equipment, such as jaw crushers, cone crushers and double-roll crushers, the crushing modes are generally considered to be static or quasi-static (Huang 2007). Research on the static and quasi-static fragmentation of ore-particle clusters is of significant importance for the development of novel and efficient comminution equipment.

This study investigates the fractal characteristics of ore-particle clusters under quasi-static loading. The Tavares model is employed to study the fragmentation characteristics of ore-particle clusters under quasi-static loading, and fractal dimension is used to analyze the degree of fragmentation in the post-crushed ore. The simulation results are validated through crushing experiments.

1. Tavares model

The Tavares model is specifically designed for simulating the fracture of granular materials. This model takes into account surface wear, strength degradation, and the overall fragmentation process of particles under external forces, providing a more realistic and comprehensive representation of the mechanisms involved in granular material fragmentation (Cleary and Sinnott 2015; Barrios et al. 2020). The Tavares model has been adapted from the original Hertz-Mindlin contact model in EDEM. Illustrated in Figure 1, the implementation of the particle fragmentation process based on the Tavares model begins with intact particles at the initial stage. When the material's energy reaches the critical value for fragmentation, the particle replacement program is invoked, removing large particles and replacing them with smaller particles. Subsequently, under the influence of contact forces, the small particles separate, resulting in the desired fragmentation effect.

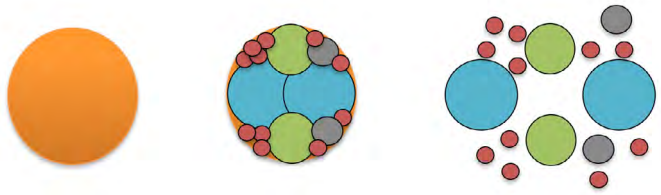

Fig. 1. Crushing process in the Tavares model

Rys. 1. Proces kruszenia w modelu Tavaresa

According to the Tavares model, the condition for the fragmentation of granular bulk materials is determined by comparing the fracture energy with the maximum fracture energy. Here, the stressing energy consists of normal energy and shear energy, as shown in Equation (1) (Tavares et al. 2021).

$$E_k = E_n + c_t E_t \tag{1}$$

↳ E_n and E_t – are the normal energy and shear energy experienced by the particles during the charging process,

c_t – shear energy coefficient.

The fracture energy of each individual particle is determined based on its size, mean value and standard deviation. This fracture energy follows an upper-truncated log-normal distribution, with the probability density function of fracture energy represented as Equation (2) (Tavares et al. 2021).

$$\begin{cases} P(E) = \dfrac{1}{2}\left[1 + erf\left(\dfrac{\ln E^* - \ln E_{50}}{\sqrt{2}\sigma}\right)\right] \\ E^* = \dfrac{E_{\max} E}{E_{\max} - E} \end{cases} \tag{2}$$

- E – the particle fracture energy distribution corresponding to the maximum stressing energy that it can sustain in a collision,
- $E_{\max}$ – denotes the upper truncation value of the log-normal distribution,
- E_{50} – represents the median fracture energy of the log-normal distribution,
- σ – the standard deviation of the log-normal distribution of fracture energy.

The median fracture energy of the particle is represented by Equation (3).

$$E_{50} = \frac{E_{\infty}}{1 + k_p / k_{st}}\left[1 + \left(\frac{d_0}{d_p}\right)^{\varphi}\right] \tag{3}$$

- E_{∞} – represents the ultimate fracture energy,
- d_0 – stands for the characteristic particle size of the granular material,
- φ – is a fitting parameter for calculating particle fracture energy,
- d_p – denotes the representative particle size of the particle size distribution,
- k_p – signifies the stiffness of the particle,
- k_{st} – represents the stiffness of the geometrical body.

If granular bulk materials do not undergo fragmentation during the loading process, the original large particle will experience damage, leading to the updating of the fracture energy of the particle. The updated fracture energy is lower than the fracture energy of the original large particle. Subsequently, upon further loading, the updating process continues until the original particle undergoes fragmentation. The relationship between the fracture energy of the particle after damage from external loading and the previous fracture energy is represented as Equation (4).

$$\begin{cases} E'_f = E_f\left(1-D\right) \\ D = \left[\dfrac{2\gamma}{\left(2\gamma-5D+5\right)}\cdot\dfrac{eE_k}{E_f}\right]^{\frac{2\gamma}{5}} \\ e = \dfrac{1}{1+k_p/k_s} \end{cases} \tag{4}$$

- E_f – fracture energy of the particle,
- E'_f – the fracture energy of the particle after damage,
- D – represents the damage coefficient, eE_k denotes the effective fracture energy,
- γ – stands for the damage accumulation coefficient,
- e – signifies the proportionality coefficient of fracture energy,
- k_p – represents the Stiffness of the particle,
- k_s – denotes the stiffness of the contact surface of the particle.

The degree of particle fragmentation can be expressed using the $t_{10} - t_n$, in which t_{10} represents the proportion of resulting smaller particles smaller than one-tenth of the size of the feed granular bulk material. The relationship between t_{10} and the fracture energy is depicted as Equation (5).

$$t_{10} = A\left[1-\exp\left(-b\frac{eE_k}{E_f}\right)\right] \tag{5}$$

- A – represents the fitting parameter obtained from experiments, which signifies the maximum achievable value of t_{10} in experiments,
- b – another fitting parameter from experiments,
- eE_k – denotes the effective fracture energy,
- e – signifies the proportionality coefficient of fracture energy,
- E_f – signifies the fracture energy of the particle.

2. Simulation and analysis of fragmentation

2.1. The simulation process of ore-particle cluster fragmentation

When conducting simulation and analysis of ore fragmentation using EDEM, it is essential to calibrate the parameters of the ore. Referring to relevant material manuals and incorporating the preliminary work experience of the project team, the intrinsic parameters of the

ore, contact mechanics parameters, and Tavares model setting parameters can be obtained. These parameters are detailed in Tables 1, 2 and 3, respectively.

Considering the ore feed size in the range of 16 to 18 mm and practical experimental conditions, the structural dimensions of the loading cylinder were selected as depicted in Figure 2. In this configuration, the inner diameter of the test cylinder is 150 mm, and its height is 125 mm. To explore the fractal characteristics of ore fragmentation under different

Table 1. Intrinsic parameters of the ore

Tabela 1. Wewnętrzne parametry rudy

Materials	Density (kg/m^3)	Shear modulus (Pa)	Poisson's ratio
Wolframite	2,830	2.5*10^10	0.25
Equipment	7,800	7.9*10^10	0.30

Table 2. Contact mechanics parameters

Tabela 2. Parametry mechaniki kontaktu

Contact parameter	Wolframite – Wolframite	Equipment – Wolframite
Coefficient of resilience	0.20	0.25
Coefficient of static friction	0.45	0.65
Coefficient of rolling friction	0.30	0.50

Table 3. Tavares model configuration parameters

Tabela 3. Parametry konfiguracji modelu Tavaresa

Damage constant	3.0
E_{50} parameter (mm)	8.0
Fitting parameter	0.84
Standard deviation of the fracture energy	0.4
alpha_percentage	49.6
b	0.025
Minimum particle size for breakage (mm)	1.00
Minimum collision energy (J)	0.0001

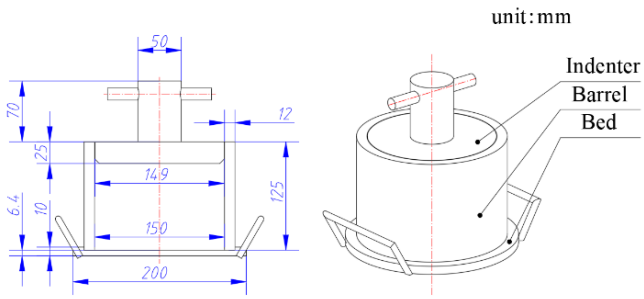

Fig. 2. Schematic diagram of the loading cylinder

Rys. 2. Schemat ideowy cylindra ładującego

loading forces and investigate the impact of varying loading forces on the fractal features of ore fragmentation, five sets of simulation experiments were designed, each representing different quasi-static loads of 100 kN, 150 kN, 200 kN, 250 kN and 300 kN.

2.2. Analysis of post-crushing particle size distribution

The simulation process of the ore-particle clusters crushing experiment obtained in EDEM post-processing is illustrated in Figure 3. It can be observed that at the initial moment of the crushing simulation, the ore-particle models are predominantly large particles. As the simulation progresses, the indenter begins its descent, leading to a gradual reduction in the gaps between ore-particle models and a decrease in the void ratio within the ore--particle clusters. Consequently, large ore particles commence the fragmentation process, ultimately yielding smaller particles.

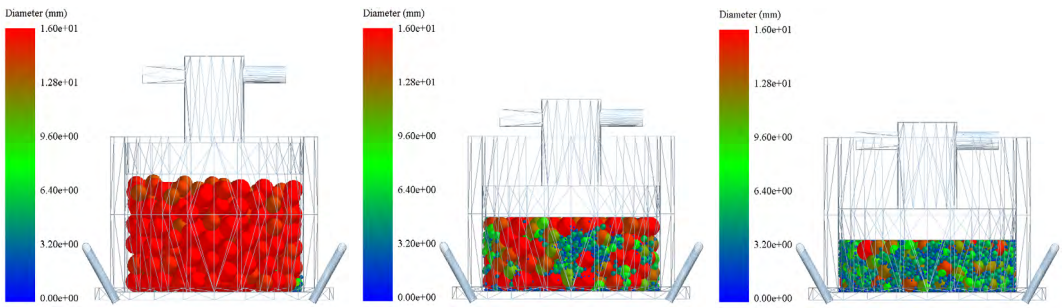

a) Initial moment b) Intermediate process c) End Time

Fig. 3. Simulation process of ore-particle clusters crushing experiment

Rys. 3. Proces symulacji kruszenia skupisk cząstek
a) Moment początkowy, b) Proces pośredni, c) Czas zakończenia

The particle size and mass information were exported during post-processing, and MATLAB software was employed for data analysis. The resulting post-crushing particle size distribution under quasi-static loading for a wolframite ore is depicted in Figure 4.

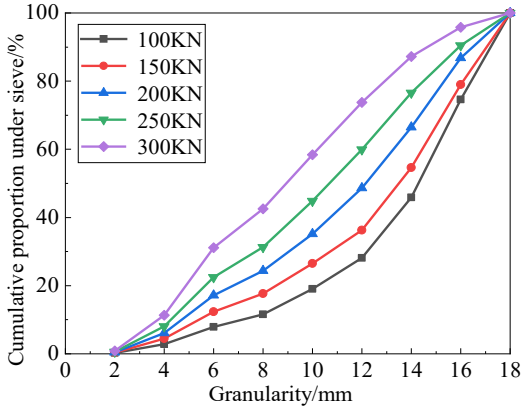

Fig. 4. Particle size distribution of a wolframite ore under quasi-static loading simulation

Rys. 4. Rozkład wielkości cząstek rudy wolframitu w symulacji obciążenia quasi-statycznego

Analysis of Figure 4 reveals distinct post-crushing particle size distributions under varying quasi-static loads. With the increase in quasi-static load, the initial slope of the particle size distribution curve steadily rises, indicating a higher proportion of smaller particles post-crushing and a greater degree of fragmentation within the ore-particle clusters. Comparative data analysis indicates that at a quasi-static load of 100 kN, the ore-particle size is predominantly comprised of large particles (diameter greater than 12 mm) and medium particles (diameter in the range 6–12 mm), accounting for 92.12% of the total. The content of small particles (diameter less than 6 mm) is relatively low. As the quasi-static load increases, the content of small particles progressively rises. When the quasi-static load reaches its maximum of 300 kN, the combined mass percentage of medium and small particles reaches 73.72%. This suggests that, under the same feed particle size conditions, higher quasi-static loads result in finer post-crushed materials.

2.3. Analysis of post-crushing average particle size

To provide a more efficient and quantitative characterization of the particle size distribution features of ore-particle clusters under quasi-static loading, the post-crushing average particle size was calculated. This quantitative approach serves to describe the impact of different quasi-static loads on the fragmentation of ore-particle clusters.

$$d = \frac{\sum d_i r_i}{\sum r_i} \tag{6}$$

- d – represents the average particle size,
- d_i – is the average particle size of crushed ore particles in each statistical size grade,
- r_i – is the mass percentage of crushed particles corresponding to d_i.

The average particle size of ore-particle clusters under quasi-static loading for different influencing factors is presented in Table 4. The data for the average particle size under various influencing factors were fitted, as illustrated in Figure 5.

Analysis of Figure 5 indicates that with the continuous increase in quasi-static load, the average particle size of ore fragmentation decreases. When the quasi-static load is 100 kN, the average fragmentation size is 13.20 mm, and when the quasi-static load reaches

Table 4. Statistical parameters of post-crushing particle sizes for ore-particle clusters

Tabela 4. Parametry statystyczne wielkości cząstek po kruszeniu dla skupisk cząstek rudy

Different Quasi-Static Loads	100 kN	150 kN	200 kN	250 kN	300 kN
Fractal Dimension	0.9205	1.0676	1.1632	1.2472	1.3603
Related Coefficient	0.9963	0.9954	0.9934	0.9887	0.9792
Average Particle Size	13.20	12.38	11.29	10.31	8.98

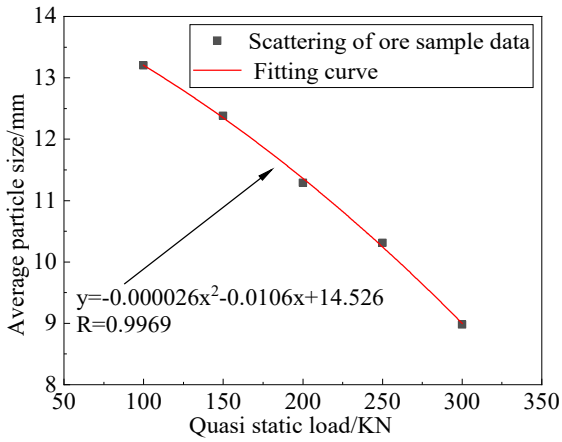

Fig. 5. Distribution of average particle size in ore-particle clusters under different quasi-static loads

Rys. 5. Rozkład średniej wielkości cząstek w skupiskach cząstek rudy przy różnych obciążeniach quasi-statycznych

300 kN, the average fragmentation size reduces to 8.98 mm. A quadratic fitting function was employed to fit the average fragmentation size data, yielding a fitting related coefficient of 0.9969, indicating high fitting accuracy. Therefore, the average fragmentation size information provides a more intuitive description of the fragmentation state of ore-particle clusters.

3. Study of fractal characteristics after crushing

3.1. Calculation of fractal dimension

There are primarily two methods for calculating the fractal dimension of ore-particle clusters: the first involves calculations based on the size-frequency relationship; the second involves calculations based on the mass-frequency relationship. Using the simulated data recorded, the mass-frequency method was employed to calculate the fractal dimension of ore-particle clusters after crushing. The particle size distribution equation (Li et al. 2019) for ore-particle clusters under quasi-static loading can be obtained as follows.

$$\frac{M(x)}{M_T} = \left(\frac{x}{x_m}\right)^{(3-D_f)} \tag{7}$$

- x – represents the size of ore particles,
- x_m – the maximum size of ore particles,
- $M(x)$ – the cumulative mass of particles with sizes less than x,
- M_T – the total mass of ore particles,
- D_fd – enotes the fractal dimension of the ore-particle clusters.

Taking the logarithm of both sides of Equation (7) yields

$$\lg\left[\frac{M(x)}{M_T}\right] = (3 - D_f)\lg\left(\frac{x}{x_m}\right) \tag{8}$$

From Equation (8), it can be observed that in the double logarithmic coordinate system with $\lg[M(x)/M_T]$ as the dependent variable and $\lg(x)$ as the independent variable, the slope of the curve obtained by fitting the discrete data using the least squares method is precisely $3 - D_f$. Thus, the fractal dimension (D_f) of the ore-particle clusters under quasi-static loading can be determined.

Using MATLAB software, the curve of the post-crushing ore-particle size distribution of ore-particle clusters under the influence of quasi-static loads is depicted in Figure 6.

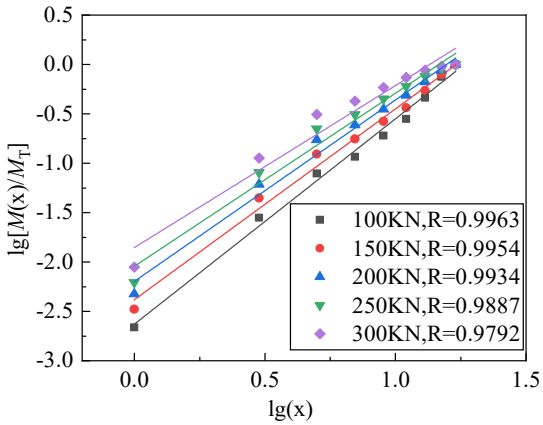

Fig. 6. lg[$M(x)/M_T$] – lg(x) curves of ore-particle cluster size distribution under different quasi-static loads

Rys. 6. lg[$M(x)/M_T$] – lg(x) krzywe rozkładu wielkości skupisk cząstek rudy przy różnych obciążeniach quasi-statycznych

Analysis of Figure 6 reveals that under different quasi-static loads, the cumulative mass percentage and post-crushing particle size of ore-particle clusters exhibit a good linear correlation in the double logarithmic coordinate system. The fractal dimension of post-crushing ore-particle clusters for different quasi-static loads are presented in Table 4. Analysis of Table 4 indicates that the fitting related coefficient of the double logarithmic relationship curves for calculating the fractal dimension of ore-particle clusters under different quasi-static loads are all greater than 0.97. This suggests that ore-particle clusters conform to fractal patterns during quasi-static loading, and the fractal dimension of ore-particle clusters under different quasi-static loads ranges from 0.9205 to 1.3603.

3.2. The relationship between fractal dimension and different quasi-static loads

Figure 7 depicts the relationship curve between fractal dimension and different quasi-static loads. Analysis of Figure 7 reveals that during the ore-crushing process, the fractal dimension increases linearly with the augmentation of quasi-static loads. The slope of the fitted curve is 0.0021 with a fitting correlation coefficient R of 0.9951, thus demonstrating a strong linear correlation. As the quasi-static load increases from 100 kN to 300 kN, the fractal dimension rises from 0.9205 to 1.3603, indicating a corresponding increase in the degree of ore crushing. Analysis indicates that increasing the quasi-static load leads to a gradual accumulation of energy at initial defects such as micro-cracks, joints, and voids within the ore. Consequently, the growth and development of initial

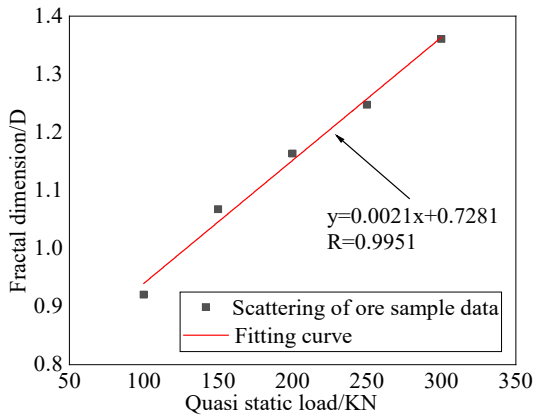

Fig. 7. Relationship curve between fractal dimension and different quasi-static loads

Rys. 7. Krzywa zależności między wymiarem fraktalnym a różnymi obciążeniami quasi-statycznymi

defects within the ore result in macroscopic fragmentation. As the number of smaller particles increases, the fractal dimension gradually enlarges, intensifying the degree of ore fragmentation.

3.3. The relationship between fractal dimension and average particle size after crushing

In order to provide a more intuitive description of the particle distribution characteristics of crushed ore under quasi-static loading conditions, the average particle size calculation method was adopted to quantitatively assess the information on particle average distribution, as explained in Section 2.3. The average particle size data was then fitted with the corresponding fractal dimension data, resulting in the relationship curve between the average particle size and fractal dimension of the crushed ore-particle clusters, as depicted in Figure 8.

Analysis of Figure 8 reveals that the fractal dimension of the crushed ore-particle clusters under quasi-static loading decreases in accordance with the increase in the average particle size. The slope of the fitted curve is –0.0997, with a fitting correlation coefficient R of 0.9880, indicating a strong linear correlation. As the average particle size of the crushed ore-particle clusters increases from 8.98 mm to 13.20 mm, the corresponding fractal dimension decreases from 1.3603 to 0.9205. The fractal dimension is closely associated with the crushing characteristics of the ore-particle clusters, indicating that a larger fractal dimension corresponds to smaller particle sizes. Therefore, the fractal dimension effectively reflects the crushing process of the ore-particle clusters. This indicates that the particle size distribution of the fragmented ore exhibits good self-similarity and significant fractal characteristics.

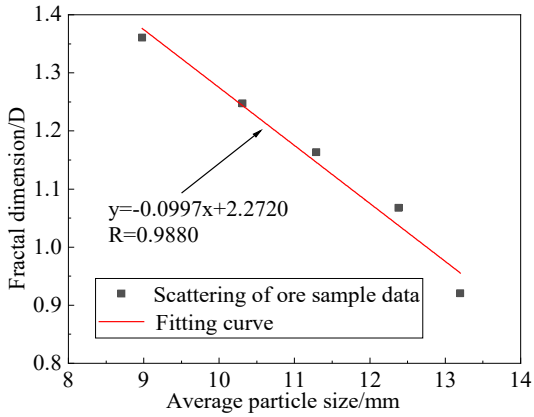

Fig. 8. Relationship curve between average particle size and fractal dimension

Rys. 8. Krzywa zależności między średnim rozmiarem cząstek a wymiarem fraktalnym

4. Experimental investigation of ore-particle clusters crushing

4.1. Experimental procedures

The quasi-static loading test of a wolframite ore was conducted using a computerized universal material testing machine (Model: WE-1000B), as illustrated in Figure 9. The experimental setup was comprised of a computer, a control cabinet, a hydraulic control system, a displacement sensor, a pressure sensor and a loading cylinder.

a) Overall Device b) Magnified View

Fig. 9. Experimental setup for quasi-static loading test of a wolframite ore

Rys. 9. Układ doświadczalny testu obciążenia quasi-statycznego rudy wolframitu

The samples used in the experiment were wolframite ore from a mine in southern Jiangxi Province, with a density of 2,740 kg/m^3. These ore samples were the products of a jaw crusher, with a particle size range of 30 to 50 mm. To meet the experimental requirements, preliminary crushing was conducted using a laboratory-scale jaw crusher. Subsequently, the crushed material was sieved to obtain experimental samples within the particle size range of 16 to 18 mm.

The experimental samples were placed into a loading pressure cylinder with a material layer height of 100 mm. They were subjected to loading using a digital display universal material testing machine, with load increments set at 100, 200 and 300 kN. The loading rate was controlled at 1 kN/s via the control console. Subsequently, unloading was performed. Each experimental set was repeated three times, resulting in a total of nine experiments.

4.2. Analysis of experimental results

After unloading with the universal material testing machine, the loading cylinder is taken out, and the ore is sieved through a screening experiment to obtain the particle size distribution of the ore with an initial particle size of 16 to 18 mm, as shown in Table 5.

The particle size distribution of the crushed ore was statistically analyzed for each experimental group. The statistical results of the average post-crushing cumulative undersize yield for wolframite ore are depicted in Figure 10.

It is evident that the trend of post-crushing proportions in the experiments closely aligns with the simulation results. Specifically, when quasi-static loads are set at 100 kN, 200 kN and 300 kN, the proportions of ore particles smaller than 6 mm are 3.98%, 10.21% and 21.77%, respectively. Compared to the simulation, the absolute errors are 3.90%, 6.98%

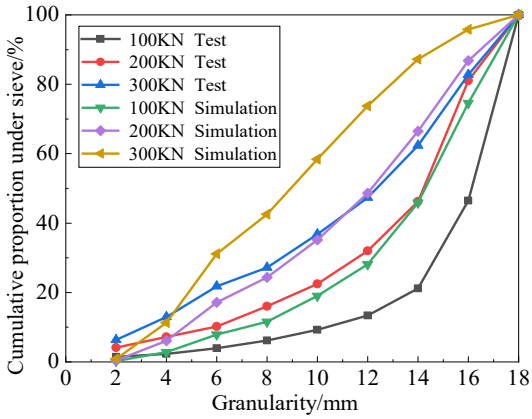

Fig. 10. Cumulative proportion under sieve

Rys. 10. Skumulowany udział pod sitem

Table 5. Sieving statistical results

Tabela 5. Wyniki statystyczne przesiewania

Number	Loading pressure (kN)		Particle size after crushing (mm)									Total
			–2	–4+2	–6+4	–8+6	–10+8	–12+10	–14+12	–16+14	–18+16	
1-1	100	Mass (g)	45	12	31	72	82	77	208	657	1,346	2,530
		Proportion (%)	1.78	0.47	1.23	2.85	3.24	3.04	8.22	25.97	53.20	100
1-2	100	Mass (g)	36	21	64	35	62	123	192	615	1,343	2,491
		Proportion (%)	1.45	0.84	2.57	1.41	2.49	4.94	7.71	24.69	53.91	100
1-3	100	Mass (g)	31	32	28	61	85	110	193	637	1,352	2,529
		Proportion (%)	1.23	1.27	1.11	2.41	3.36	4.35	7.63	25.19	53.46	100
2-1	200	Mass (g)	95	93	61	157	179	211	364	887	481	2,528
		Proportion (%)	3.76	3.68	2.41	6.21	7.08	8.35	14.40	35.09	19.03	100
2-2	200	Mass (g)	104	69	98	147	144	260	334	867	466	2,489
		Proportion (%)	4.18	2.77	3.94	5.91	5.79	10.45	13.42	34.83	18.72	100
2-3	200	Mass (g)	111	70	68	137	161	244	372	867	484	2,514
		Proportion (%)	4.42	2.78	2.70	5.45	6.40	9.71	14.80	34.49	19.25	100
3-1	300	Mass (g)	131	215	293	85	264	235	336	480	450	2,489
		Proportion (%)	5.26	8.64	11.77	3.42	10.61	9.44	13.50	19.28	18.08	100
3-2	300	Mass (g)	168	144	284	121	245	260	400	498	426	2,546
		Proportion (%)	6.60	5.66	11.15	4.75	9.62	10.21	15.71	19.56	16.73	100
3-3	300	Mass (g)	184	139	88	203	222	302	398	572	426	2,534
		Proportion (%)	7.26	5.49	3.47	8.01	8.76	11.92	15.71	22.57	16.81	100

and 9.36%, respectively. The main source of error lies in the influence of the external appearance of the ore on the crushing effect.

Conclusions

1. Under the influence of different quasi-static loads, the distribution of crushed particle sizes varies significantly. With the gradual increase in quasi-static load, the proportion of smaller particles after crushing becomes higher, indicating a greater degree of fragmentation in the ore-particle clusters.
2. With the continuous increase in quasi-static load, the average particle size of the crushed ore shows a decreasing trend. When the quasi-static load is 100 kN, the average crushed particle size is 13.20 mm. As the quasi-static load reaches 300 kN, the average crushed particle size decreases to 8.98 mm. The information on average crushed particle size provides an intuitive description of the ore crushing condition.
3. The ore-particle clusters exhibit fractal patterns during quasi-static loading, with the fractal dimension ranging from 0.9205 to 1.3603 under different quasi-static loads. As the quasi--static load increases, the fractal dimension also increases. In the transition from 100 kN to 300 kN quasi-static load, the fractal dimension increases from 0.9205 to 1.3603, indicating a corresponding increase in the degree of ore fragmentation. Additionally, the fractal dimension decreases with the increase in the average particle size of the crushed ore. When the average particle size of the ore-particle clusters increases from 8.98 mm to 13.20 mm, the corresponding fractal dimension decreases from 1.3603 to 0.9205.

This work was supported by the National Natural Science Foundation of China grant 52364025.

REFERENCES

Barrios et al. 2020 – Barrios, G., Jiménez-Herrera, N. and Tavares, L.M. 2020. Simulation of particle bed breakage by slow compression and impact using a DEM particle replacement model. *Advanced Powder Technology* 31(7), pp. 2749–2758, DOI: 10.1016/j.apt.2020.05.011.

Cleary, P.W. and Sinnott, M.D. 2015. Simulation of particle flows and breakage in crushers using DEM: Part 1 – Compression crushers. *Minerals Engineering* 74, pp. 178–197, DOI: 10.1016/j.mineng.2014.10.021.

Cai et al. 2016 – Cai, G.P., Xiao, X.H., Xu, Q. and Shen, J. 2016. Establishing Low-frequency Vibration Extrusion Crushing Energy Consumption Prediction Expression Based on Fractal Theory. *Nonferrous Metals (Mineral Processing Section)*, pp. 58–62 (*in Chinese*).

Evertsson, C.M. and Bearman, R.A. 1997. Investigation of interparticle breakage as applied to cone crushing. *Minerals Engineering* 10(2), pp. 199–214, DOI: 10.1016/S0892-6875(96)00146-X.

Huang, D.M. 2007. Research on Working Mechanism and Working Performance Optimization of Compressive Crusher. *Shanghai Jiao Tong University* (*in Chinese*).

Jiménez-Herrera et al. 2017 – Jiménez-Herrera, N., Barrios, G. and Tavares, L.M. 2017. Comparison of breakage models in DEM in simulating impact on particle beds. *Advanced Powder Technology* 29(3), pp. 692–706, DOI: 10.1016/j.apt.2017.12.006.

Liu, J. and Schönert, K. 1996. Modelling of interparticle breakage. *International Journal of Mineral Processing* 44–45, pp. 101–115, DOI: 10.1016/0301-7516(95)00022-4.

Liu et al. 2005 – Liu, H.Y., Kou, S.Q. and Lindqvist, P.A. 2005. Numerical studies on the inter-particle breakage of a confined particle assembly in rock crushing. *Mechanics of Materials* 37(9), pp. 935–954, DOI: 10.1016/j.mechmat.2004.10.002.

Liu et al. 2013 – Liu, S., Xu, J.Y., Bai, E.L. and Gao, Z.G. 2013. Research on impact fracture of rock based on fractal theory. *Journal of Vibration and Shock* 32(05), pp. 163–166 (*in Chinese*).

Li et al. 2019 – Li, C.J., Xu, Y., Zhang, Y.T. and Li, H.L. 2019. Study on energy evolution and fractal characteristics of cracked coal-rock-like combined body under impact loading. *Chinese Journal of Rock Mechanics and Engineering* 38(11), pp. 2231–2241 (*in Chinese*).

Liu, R.Y. 2020. Study on mechanism and performance evaluation of cone crusher. *University of Science and Technology Beijing* (*in Chinese*).

Nguyen et al. 2002 – Nguyen, A.Q., Husemann, K. and Oettel, W. 2002. Comminution behaviour of an unconfined particle bed. *Minerals Engineering* 15(1–2), pp. 65–74, DOI: 10.1016/S0892-6875(01)00201-1.

Ning et al. 2018 – Ning, S., Yang, Y.L., Lv, J.K. and Duan, H.Q. 2018. The Fractal Characteristics of Coal Sample's Fragments Subjected to Cyclic Loading. *Geotechnical and Geological Engineering* 37(15), pp. 2267–2281, DOI: 10.1007/s10706-018-0735-0.

Tavares et al. 2021 – Tavares, L.M., Rodriguez, V.A., Sousani, M., Padros, C.B. and Ooi, J.Y. 2021 An effective sphere-based model for breakage simulation in DEM. *Powder Technology* 392, pp. 473–488, DOI: 10.1016/j.powtec.2021.07.031.

Wu, R.J. and Li, H.B. 2019. Multi-scale failure mechanism analysis of layered phyllite subject to impact loading. *Explosion and Shock Waves* 39(190), pp. 108–117, DOI: 10.11883/bzycj-2019-0187 (*in Chinese*).

Wang, Y.X. and Liang, W.M. 2020. Fractal Study on Influence of Impact Load on Microscopic Pore of Anthracite. *Chinese Journal of High-Pressure Physics* 34(157), pp. 134–144 (*in Chinese*).

Zhang et al. 2017 – Zhang, Z.L., Ren, T.Z., Cheng, J.Y. and Jin, X. 2017. Research on the Inter-particle Breakage of Cone Crusher Considering the Characteristics of Particle Shape Transformation. *Journal of Mechanical Engineering* 53(16), pp. 173–180 (*in Chinese*).

Zhang et al. 2017 – Zhang, Z.L., Ren, T.Z., Cheng, J.Y. and Jin, X. 2017. The improved model of inter-particle breakage considering the transformation of particle shape for cone crusher. *Minerals Engineering* 112, pp. 11–18.

FRACTAL CHARACTERISTICS ANALYSIS OF ORE PARTICLE CLUSTERS UNDER QUASI-STATIC LOADING

Keywords

fractal dimension, ore particle clusters, fracture characteristics, Tavares model, wolframite

Abstract

To investigate the quasi-static loading fracture characteristics of a certain wolframite ore, a crushing model of ore particle clusters was established using the Tavares model. The fracture characteristics of ore particle clusters under quasi-static loading were studied through simulation, and the results were compared with experimental data from crushing tests. The findings revealed that under different quasi-static loads, the post-crushing particle size distribution varied significantly. With increasing quasi-static loads, the proportion of smaller particles after crushing increased, indicating a higher degree of fragmentation in the ore particle clusters. Additionally, as the quasi-static load continued to increase, the average particle size of the ore particle clusters decreased. The average

particle size provided a direct and intuitive measure of the fragmentation status of the ore particle clusters. Furthermore, the ore particle clusters exhibited fractal patterns during quasi-static loading, with the fractal dimension of particle size distribution ranging from 0.9205 to 1.3603 under different quasi-static loads. The fractal dimension increased with the increment of quasi-static load, indicating a higher level of fragmentation. Moreover, the fractal dimension of ore particle clusters during quasi-static loading exhibited a decreasing trend with the average particle size of fragmentation. This study contributes to a comprehensive understanding of the fractal characteristics associated with the quasi-static loading fracture of ore particle clusters.

ANALIZA CHARAKTERYSTYK FRAKTALNYCH SKUPISK CZĄSTEK RUDY POD OBCIĄŻENIEM QUASI-STATYCZNYM

Słowa kluczowe

wymiar fraktalny, skupiska cząstek rudy, charakterystyka pęknięć, model Tavaresa, wolframit

Streszczenie

Aby zbadać charakterystykę pękania pod obciążeniem quasi-statycznym określonej rudy wolframitu, opracowano model kruszenia skupisk cząstek rudy przy użyciu modelu Tavaresa. Charakterystykę pękania skupisk cząstek rudy pod obciążeniem quasi-statycznym zbadano poprzez symulację, a wyniki porównano z danymi eksperymentalnymi z testów kruszenia. Wyniki badań wykazały, że przy różnych obciążeniach quasi-statycznych rozkład wielkości cząstek po kruszeniu znacznie się różnił. Wraz ze wzrostem obciążeń quasi-statycznych zwiększał się udział mniejszych cząstek po kruszeniu, co wskazuje na wyższy stopień rozdrobnienia skupisk cząstek rudy. Dodatkowo, w miarę dalszego wzrostu obciążenia quasi-statycznego, średni rozmiar cząstek w skupiskach cząstek rudy zmniejszał się. Średni rozmiar cząstek stanowił bezpośrednią i intuicyjną miarę stanu rozdrobnienia skupisk cząstek rudy. Co więcej, skupiska cząstek rudy wykazywały fraktalne wzory przy quasi-statycznym obciążeniu, z fraktalnym wymiarem rozkładu wielkości cząstek w zakresie od 0,9205 do 1,3603 przy różnych obciążeniach quasi-statycznych. Wymiar fraktalny wzrastał wraz ze wzrostem obciążenia quasi-statycznego, wskazując na wyższy stopień kruszenia. Co więcej, wymiar fraktalny skupisk cząstek rudy podczas quasi-statycznego obciążenia wykazywał tendencję malejącą wraz ze średnim rozmiarem cząstek kruszenia. Badanie to przyczynia się do wszechstronnego zrozumienia charakterystyki fraktalnej związanej z quasi-statycznym pękaniem obciążeniowym skupisk cząstek rudy.